J. Amer. Soc. Hort. Sci. 146(4):241–251. 2021. https://doi.org/10.21273/JASHS05027-20

A High-throughput Color Measurement System for Evaluating Flesh Browning in Apples

Taku Shimizu
Division of Apple Research, Institute of Fruit Tree and Tea Science, National Agriculture and Food Research Organization (NARO), 92-24 Nabeyashiki, Shimokuriyagawa, Morioka, Iwate 020-0123, Japan; and Faculty of Agriculture Department of Plant Bioscience, Iwate University, 3-18-8 Ueda, Morioka, Iwate 020-8550, Japan

Kazuma Okada
Division of Fruit Breeding and Genomics, Institute of Fruit Tree and Tea Science, NARO, 2-1 Fujimoto, Tsukuba, Ibaraki 305-8604, Japan

Shigeki Moriya
Division of Apple Research, Institute of Fruit Tree and Tea Science, National Agriculture and Food Research Organization (NARO), 92-24 Nabeyashiki, Shimokuriyagawa, Morioka, Iwate 020-0123, Japan

Sadao Komori
Faculty of Agriculture Department of Plant Bioscience, Iwate University, 3-18-8 Ueda, Morioka, Iwate 020-8550, Japan

Kazuyuki Abe
Division of Fruit Breeding and Genomics, Institute of Fruit Tree and Tea Science, NARO, 2-1 Fujimoto, Tsukuba, Ibaraki 305-8604, Japan

Additional index words. apple fruit, browning index, color difference, colorimetry, digital image analysis

Abstract. **The development of new high-quality apple (*Malus* ×*domestica*) cultivars that are resistant to flesh browning is needed to expand the use of apples in the food service and catering industry. However, conventional methods for evaluating apple flesh browning can be both time-consuming and costly, thereby rendering such methods unsuitable for breeding programs that must characterize a large number of product samples. Therefore, it is necessary to develop new, simple, and inexpensive methods. The aim was to develop a method for simultaneously measuring the color values of 42 apple samples using a digital camera. The processing time per sample was reduced to less than one-tenth of that of the conventional method. The measurement dispersion [SD of the color difference between two colors (ΔE^*_{ab})] of this system was less than 0.08, equivalent to the nominal value of a general colorimeter. Time-series analysis of six apple cultivars using this method showed that the calculated browning index values correlated well with the degree of browning judged by human perception. Further, the measurement data showed that the CIE *L* a* b** value trends associated with browning in reddish- and watercored-flesh samples, was different from the corresponding trends in yellowish-flesh samples. This work reports the development of a high-throughput analytical system of apple browning and provides cautionary notes for evaluating reddish- and watercored-flesh browning, which should be measured on a different basis from that used for normal-flesh browning.**

The processing of fresh-cut fruits has increased their consumption because of the ease and variety of their use in the food service industry (Lu et al., 2007; Oliveira et al., 2015); however, the processing of several kinds of fruits and vegetables, including apple (*Malus* ×*domestica*), causes their surfaces to turn a brownish color (Pristijono et al., 2006). These color changes (hereinafter referred to as "browning") are caused by phenolic oxidation reactions catalyzed by polyphenol oxidases, such as tyrosinases and laccases (Veltman et al., 1999). The quality of the taste and aroma of apples deteriorates with browning (Coseteng and Lee, 1987; Guardo et al., 2013; Murata et al., 1995); therefore, an extra step during processing, namely, coating with an antioxidant, is required to control the damage. For these reasons, apples have limited use in the food service and catering industries, compared with other fruits, such as citrus (*Citrus* sp.), grape (*Vitis* sp.), and pineapple (*Ananas comosus*). The use of nonbrowning apple cultivars may increase the demand and consumption of fresh-cut apples, but only a few such cultivars exist. 'Aori27' (Igarashi et al., 2016; Tazawa et al., 2019) and Arctic™ apples (Carter, 2012) are genetically modified cultivars that show natural browning resistance. Increasing the number of nonbrowning cultivars would increase fresh-cut apple availability. To develop them, it would be useful to obtain information on the degree of

Received for publication 7 Dec. 2020. Accepted for publication 23 Feb. 2021. Published online 11 May 2021.
We thank Dr. Chikako Honda for his helpful advice to improve the application of the measurement system.
T.S. is the corresponding author. E-mail: takushimizu@affrc.go.jp.

browning among cultivars, but apple flesh coloration is not consistent across cultivars.

Some cultivars have reddish flesh that becomes darker when exposed to air. In addition, watercore, in which part of the flesh appears translucent and water-soaked, may develop in late-harvested apples. Watercore in fruit such as fully ripe 'Fuji' apples is popular in Japan (Arakawa and Komori, 2006), although it is generally treated as an internal physiological disorder because it shortens shelf life (Bennedsen and Peterson, 2005). Studies examining reddish and watercored flesh are limited because these specialized tissues are usually patchy and it is therefore difficult to evaluating browning using conventional methods, such as colorimetry or measuring polyphenol oxidase activity and polyphenol composition.

Moreover, general methods for measuring food browning are not suitable for measuring a large number of samples because these methods only measure one sample at a time, making them both time-consuming and costly. In addition, many other farm products, such as european pear (*Pyrus communis*), peach (*Prunus persica*), eggplant (*Solanum melongena*), globe artichoke (*Cynara scolymus*), and mushroom (*Agaricus bisporus*), undergo color changes (Amiot et al., 1995; Cabezas-Serrano et al., 2009; Lee et al., 1990; Prohens et al., 2007; Quevedo et al., 2016). An efficient and easy-to-use color evaluation method may be applicable to other crops. A more effective method for evaluating browning is needed for selecting nonbrowning apple cultivars.

Color gamut measurement is a technique that uses computer imaging systems and color images from digital cameras or scanners in addition to colorimetry (León et al., 2006; Yam and Papadakis, 2004). A color gamut is measured in a given region of the sample image [i.e., the region of interest (ROI)] to analyze the color of multiple samples at one time. Previous reports have proposed similar colorimetric systems, and their advantages have been discussed (León et al., 2006; Quevedo et al., 2014). For example, these systems can observe color changes in a time-dependent, nondestructive, and noninvasive manner that can detect even subtle changes in fruit coloration. However, these systems either do not consider the measurement error that arises from differences in brightness owing to sample position, or they correct for this error using a colorimeter. Correcting for these errors without using a colorimeter may simplify the system and facilitate its broader use. In addition, these systems imitate the measuring method of a colorimeter, and one of the features is that they make an adequate substitute for an expensive and high-performance device. However, recently, colorimeters such as the Nix Pro 2 Color Sensor (Nix Sensor, Hamilton, ON, Canada), which are very inexpensive ($349) and have sufficient accuracy for scientific measurement (Hodgen, 2016; Holman et al., 2018; Stiglitz et al., 2016), have become available. It is necessary to carefully consider the advantages and disadvantages of each method after comparing it with such products.

The ΔL^*, Δa^*, and Δb^* indices represent changes in the L^* (the color parameter for lightness), a^* (the color parameter for greenness to redness), and b^* (the color parameter for blueness to yellowness) values in the CIE 1976 L^* a^* b^* color space (Robertson, 1977). ΔE^*_{ab}, which is often used to quantify the difference between two colors, is calculated from two coordinates of difference in the L^* a^* b^* color space using the following equation:

$$\Delta E^*_{ab} = \sqrt{(L^* - L^{*\prime})^2 + (a^* - a^{*\prime})^2 + (b^* - b^{*\prime})^2} \quad [1]$$

These values have been used to evaluate fresh-cut apple browning; however, Lunadei et al. (2011) and Quevedo et al. (2009) suggest that there are other indices that better explain the degree of fruit browning. Potential useful indicators include the browning index [BI (Buera et al., 1985; Lunadei et al., 2010)], which represents the degree of browning in a variety of foods, and the CIE DE2000 color difference [ΔE_{00} (Luo et al., 2001)], which is an index adjusted for ΔE^*_{ab} to suit human perception. It is important to quantify the degree of browning using these indices because they are expected to represent apple flesh browning better than any L^* a^* b^* indices.

Here, we aimed to select an index that enables accurate browning evaluation for any type of apple flesh to allow the accurate evaluation of hybrid progenies with a variety of flesh colors. The objective of this study was to develop a high-throughput, cost-effective analytical system to measure apple browning with a small measurement error. Thus, we attempted 1) to develop a method for the simultaneous measurement of many samples without a colorimeter or other expensive devices; 2) to establish an evaluation index to identify the ideal degree of apple flesh browning; 3) to establish a high-throughput system to determine the degree of apple flesh browning using this method; and 4) to investigate the parameters required to quantify apple browning in cultivars with uncommon flesh colors.

Materials and Methods

Plant material. Ten apple cultivars and one hybrid progeny were used in the experiments: two severely browning cultivars—Fuji (FJ) and Cripps Pink (CP); three mildly browning cultivars—Shinanogold (SG), Kinshu (KS), and Tsugaru (TG); one browning-resistant cultivar—Aori27 (AO); four reddish-flesh cultivars—Geneva (GN), Pink Pearl (PP), Rose Pearl (RP), and Ruby Sweet (RS); and one watercored hybrid progeny—7-10011 [Haruka × Aika-no-kaori (PG)]. All materials were planted in the experimental orchard at the Apple Research Station, National Agriculture and Food Research Organization (Morioka, Japan). The experiments were conducted in 2017 and 2018.

Apple flesh samples. Six (for measurement conditions) or three (other experiments) ripe fruit were harvested from the same tree for each cultivar and the hybrid progeny, and stored at 1 °C for at least 16 h and up to 4 weeks before use. Only one sample was prepared from each fruit. The sunlit side of each fruit was vertically sliced into 3-mm-thick samples using a stainless-steel vegetable slicer. These slices were further processed into 40-mm-diameter samples cut from the slice interior using a circular cutting die. The flesh disks obtained were placed at 42 measuring points on an acrylic board (Fig. 1A). The first measurement was taken within about 5 min of the start of sample preparation. If the color of the sample changed significantly (ΔE_{00} at 5 min after the start of preparation was more than 1.0), the first measurement was taken within 1.5 min after the start of preparation. We also used grated apple flesh samples for measurement to compare the coloration trends to the sliced samples. The grated samples were prepared after removing the core and pericarp from 100 g of fruit. The samples were processed using a stainless-steel grater and placed on glass laboratory dishes. The first measurement was taken within 1.5 min of

sample preparation. The grated samples were measured one at a time.

Color standards. One hundred and forty color standards (Supplemental Table 1) were selected from a commercial formula guide kit (Pantone Formula Guide Solid Coated & Uncoated; Pantone, Carlstadt, NJ) and used for calibration (Fig. 1B).

Lighting system. A camera and four D65 fluorescent lamps (FL20S·D-EDL-D65; Toshiba, Tokyo, Japan) with a color temperature of 6504 K and a color index (Ra) close to 98, were placed in a light booth. A diffusion light reflector made of foam-core board covered with neutral drawing paper (Luminescence neutral white; Tokushu Tokai Paper Co., Shimada, Japan) was used to light the sample area uniformly (Fig. 2). A digital camera (E-510; Olympus, Tokyo, Japan) and interchangeable lens (EZ-1442, Olympus) were fixed vertically over a gray background at 0.45 m. The zoom lens was fixed at a 75° view angle, and the camera optimum exposure and white balance settings were determined with a silk gray card (version 2; Ginichi, Tokyo, Japan). All settings were set manually (Table 1). The camera used a self-timer function. Forty-two samples were placed in the image-capture area of the camera. The light booth was located in a room without any external light; the room temperature (20 °C) and relative humidity (80%) were fixed. The apple disk samples were photographed seven (reddish and watercored flesh) or 20 (normal flesh) times over 24 h. The grated apple samples were photographed 25 times over 60 min.

Calibration and color measurement. The digitized images were transferred to a personal computer using a memory card (Compact Flash; Western Digital Corp., San Jose, CA) and transformed to an 8-bit TIFF format in the standard color space [sRGB IEC61966-2.1 (International Electrotechnical Commission, 1999)] using the image organizer software (Photoshop Lightroom CC; Adobe, San Jose, CA). The "Profile Correction" and "Remove Chromatic Aberration" functions were selected after the photographs were converted. The following methods describe the background correction and RGB calibration that were applied to each of the 42 measurement points.

Sample color extraction. Image analysis was performed using an image processing program (ImageJ, version 1.52; National Institutes of Health, Bethesda, MD) and operated with a macro file that performs a loop handling of the "RGB Measure" plugin. Forty-two circles with diameters of 215 pixels were created over the sample ROIs using the "ROI Manager" tools, with one additional ROI for background correction. Then, the mean intensity values for red, green, and blue (***R***, ***G***, ***B***) in each ROI were extracted with the "RGB Measure" plugin.

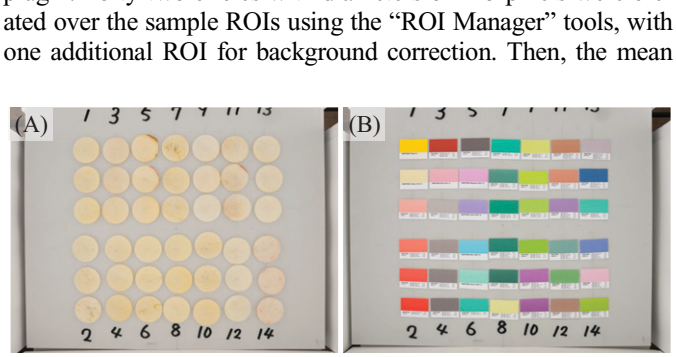

Fig. 1. The sample arrangements for calibration and color measurement. (**A**) Apple flesh samples and (**B**) color standards (Formula Guide Solid Coated & Uncoated; Pantone, Carlstadt, NJ) were arranged and photographed as the same 42 points installed on a gray acrylic board. The numbers on the acrylic board were used as a guide for the sample position and are not related to the measurement.

Background correction. Corrected intensities were calculated to offset brightness differences in each image. An additional ROI was treated as a reference measurement point and installed on the background of the measurement area. The corrected intensity values at the i^{th} measurement point in the t^{th} image were as follows:

$$I^{C}_{i,t} = I_{i,t} - \left(I^{ref}_{t} - I^{ref}_{1}\right), \quad [2]$$

where I is the measured intensity value of R, G, or B, and I^{ref} is the measured value of the reference ROI.

RGB calibration. Calibration was performed using color standards to correct errors in different measurement points owing to the lighting system and camera structure. The R, G, B values of the color standards in the sRGB color space were obtained from the color management software (PSC-CM100; Pantone) and treated as color-intensity values for the color standards used. The measurement and background correction methods used for the fruit samples were also used to perform the actual measurements of the R^C, G^C, and B^C values of the color standards. These two sets of values (e.g., standard and measured) were fitted to a three-way smoothing spline analysis of variance (SSANOVA) regression model:

$$I^{std}_{i,\ j} = \eta(x_{i,j}) + \varepsilon_{i,j}\ , \quad [3]$$

where $I^{std}_{i,j}$ is the R, G, or B intensity of the i^{th} standard color at the j^{th} measurement. The function η is decomposed into the following main and interaction effects:

$$\begin{aligned}\eta(x_{i,j}) = {} & \eta_0 + \eta_1(R_{i,j}) + \eta_2(G_{i,j}) + \eta_3(B_{i,j}) \\ & + \eta_{12}(R_{i,j}, G_{i,j}) + \eta_{23}(G_{i,j}, B_{i,j}) \\ & + \eta_{13}(B_{i,j}, R_{i,j}) + \eta_{123}(R_{i,j}, G_{i,j}, B_{i,j})\ , \end{aligned} \quad [4]$$

where η_0 is a constant function, η_1 is the main effect of R intensity, η_2 is the main effect of G intensity, η_3 is the main effect of B intensity, η_{12} is the R-G interaction effect, η_{23} is the G-B interaction effect, η_{13} is the B-R interaction effect, and η_{123} is the R-G-B three-factor interaction effect. The SSANOVA fitted values can be written as:

$$\hat{\eta}(x) = \sum_{k=1}^{p} \hat{\beta}_k f_k(x)\ , \quad [5]$$

where $f_k(x)$ is the B-spline basis function, and $\hat{\beta}_k$ is the estimated regression coefficient.

The SSANOVA process was implemented using the "ssanova" function in the R package "gss". The smoothing parameters of these models were selected to minimize the generalized cross-validation score. Models that estimated SSANOVA were used for the calibration of the R, G, B values. If the calibrated values were beyond the range of 0 to 255, they were handled as 0 or 255.

Color space conversion. To transform the R, G, B values to L, a^*, b^*, the methods described in Hunt and Pointer (2011) and León et al. (2006) were followed, using a spreadsheet (Excel 2019; Microsoft, Redmond, WA) and the event-driven programming language (Visual Basic for Applications 7.1, Microsoft). The transformation method was applied to all the measured and calibrated sample data.

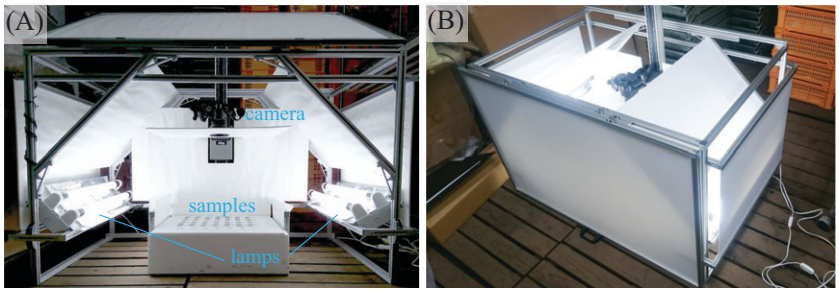

Fig. 2. Lighting system for photographing samples under stable light conditions. (**A**) Fluorescent lights were installed at positions where apple flesh and color standard samples (Formula Guide Solid Coated & Uncoated; Pantone, Carlstadt, NJ) were not directly illuminated. (**B**) The door of the lighting booth was closed at the time of sample imaging.

Browning evaluation. The color difference formulae of ΔE_{00} and ΔBI were calculated from the L^*, a^*, b^* values. The formula for calculating ΔE_{00} is defined as:

$$\Delta E_{00} = \sqrt{\left(\frac{\Delta L'}{k_L S_L}\right)^2 + \left(\frac{\Delta C'}{k_C S_C}\right)^2 + \left(\frac{\Delta H'}{k_H S_H}\right)^2 + R_T\left(\frac{\Delta C'}{k_C S_C}\right)\left(\frac{\Delta H'}{k_H S_H}\right)}, \quad [6]$$

where L' is lightness, C' is chroma, H' is hue, and S_L, S_C, and S_H are the weighting functions. In addition, R_T is a rotation function for improving the prediction of the problematic blue region. k_L, k_C, and k_H are unity values (= 1). Each parameter was calculated according to the definition described in Luo et al. (2001). The BI was calculated using the following formula:

$$BI = 100 \times \frac{X - 0.31}{0.172}, \quad [7]$$

where

$$X = \frac{a^* + 1.75L^*}{5.645L^* + a^* - 3.012b^*}.$$

The ΔBI was calculated using the following formula:

$$\Delta BI = BI' - BI. \quad [8]$$

ΔE_{00} and ΔBI were calculated using the first measurement values and each measurement; then, their maximum values (ΔE_{00max} and ΔBI_{max}) were treated as the browning scores for each cultivar.

Measurement accuracy and reproducibility. To assess the accuracy of the method, the L^*, a^*, b^* values of 51 selected color standards [different from those used for calibration (Supplemental Table 1)] were measured using a colorimeter (NF333; Nippon Denshoku Industries Co., Tokyo, Japan) and estimated using the method described previously. The accuracy was evaluated using the root mean square error (RMSE) scores of the colorimeter values, which indicated the magnitude of the difference between the values extracted from the digital images of each color sample, or the values following calibration, and the values measured by the colorimeter (Supplemental Table 2). In other words, the smaller the RMSE value, the more accurate the measurements.

To verify the effectiveness of the calibration method, the calibrated values were compared with the raw measured values and the colorimeter values. The color standard [425U, Pantone (R, G, B = 124, 126, 127)] was measured 30 times at all 42 points every 30 s. Then, the L^*, a^*, b^* values of the 42 measurement points in the 30 replicates were estimated. Finally, the ΔE^*_{ab} between the mean L^*, a^*, b^* values of the 30 replicates and each measurement were calculated.

Observation of browning in reddish flesh and watercore regions of apples from a variety of genotypes. After obtaining digital images of slice samples from reddish-flesh cultivars, the strongly reddish and pale regions of each sample were selected by appearance and set as ROIs, and named deep red (Dr) or pale red (Pr), respectively. Then, the L^*, a^*, b^* values of the Dr and Pr regions were measured and their browning values calculated. The corresponding values of watercored regions (Wc) were also measured using this method. These scores were compared with those of normal-flesh samples of FJ. The appropriateness of these browning indicators was verified with frequently used browning indices (i.e., L^*, a^*, b^*, ΔE_{00}, BI, ΔBI).

Table 1. Digital camera settings used to evaluate apple browning.

Variable	Value
Pixel resolution	3648 × 2736
Focal length	14 mm
Focus mode	Manual
Aperture	f/10
Shutter speed	1/20 s
ISO	100
Metering	Center-weighted
White balance	Preset manual
Quality	Raw
Picture mode	Muted
Noise reduction	Off
Self-timer	2 s

Results

Method for the evaluation of the degree of apple browning. A photography booth using indirect illumination, with reference to Yamamoto et al. (2011) (Fig. 2A), reduced the brightness difference in the images to one-fifth or less of the methods described by León et al. (2006) and Lv et al. (2009) (Supplemental Fig. 1). The use of a digital camera made it possible to measure multiple samples simultaneously using a simple operation and to observe time-course color changes. Moreover, by using a replaceable acrylic plate as a sample holder, more than 42 samples, which was the maximum number of simultaneous measurements, could be easily handled. The cost of making this measurement system, including the digital camera, was ≈$1900. This is more than five times the cost of an inexpensive colorimeter [i.e., Nix Pro 2 ($349)], but it is less than one-third the cost of a sophisticated colorimeter [i.e., CR-410; Konica Minolta, Tokyo, Japan ($7000)]. A comparison between our method and a commercial colorimeter is shown in Table 2.

As apple samples, we used apple flesh disks processed using a vegetable slicer and a circular cutting die (Fig. 1A). Sample preparation using this process took an average of 8.5 s per

sample. This was a 10-fold increase in efficiency compared with the preparation of 100 g of grated flesh, which took an average of 90 s. The flesh disks of six cultivars were measured 20 times between sample preparation and 24 h after processing. ΔE_{00} and ΔBI changed in a similar manner in all six cultivars (Fig. 3D–E); furthermore, these changes were in agreement with the degree of color change that was visually recognized (Fig. 3G). Although the maximum value of the indices varied with cultivar, the variation in the indices after the maximum values were obtained was slight. Based on these results, we measured the browning of apple flesh slices eight times within 24 h (at 0, 5, and 15 min, and at 1.5, 4, 7, 12, and 24 h); the maximum value of the observed index was treated as the representative value of browning degree.

Accuracy and reproducibility of the developed color measurement system. From the L^* (Fig. 4A) and b^* (Fig. 4C) values, we found that the RMSE scores of the calibrated data were smaller than those of the raw measured data at any measurement point. Overall, 5-fold or larger differences in the RMSE scores of the L^* values before (RMSE scores calculated at each of the 42 measurement points ranged from 10.806–14.297, Supplemental Table 2) and after (1.786–1.975) calibration were reported. However, for the a^* values were observed for any of the 42 measurement points compared with the other measurement points (Supplemental Table 2).

The SD of 30 replicates for each of the 42 points is shown in Fig. 4D. The SD of the calibrated data decreased significantly to approximately half of the SD of the raw data, except for one

Table 2. Comparison of the features of the developed method of evaluating apple browning with those of an inexpensive colorimeter [Nix Pro 2 (Nix Sensor, Hamilton, ON, Canada)], and two sophisticated colorimeters [CR-410 (Konica Minolta, Tokyo, Japan) and NF 333 (Nippon Denshoku Industries Co., Tokyo, Japan)]. The measured repeatability and interinstrument agreement were measured using a color standard (425U; Pantone, Carlstadt, NJ). Both ΔE^*_{ab} and ΔE_{00} are calculated from the CIE 1976 L^* a^* b^* coordinates, but in most cases ΔE^*_{ab} is slightly higher.

	Our system	Nix Pro 2	CR-410	NF 333
Monetary cost	$1,900	$349	$7,000	$7,700
Efficiency (samples/measurement)	1–42	1	1	1
Repeatability (SD of ΔE^*_{ab})	0.0767 (Measured value)	$\Delta E_{00} \leq 0.30$ (Nominal value)	≤ 0.07 (Nominal value)	0.0957 (Measured value)
Interinstrument agreement	0.776 (Measured value)	$\Delta E_{00} \leq 0.75$ (Nominal value)	≤ 0.8 (Nominal value)	No description
Measurement area	arbitrary	φ 14 mm	φ 50 mm	φ 8 mm
Output data	Image	Numeric	Numeric	Numeric

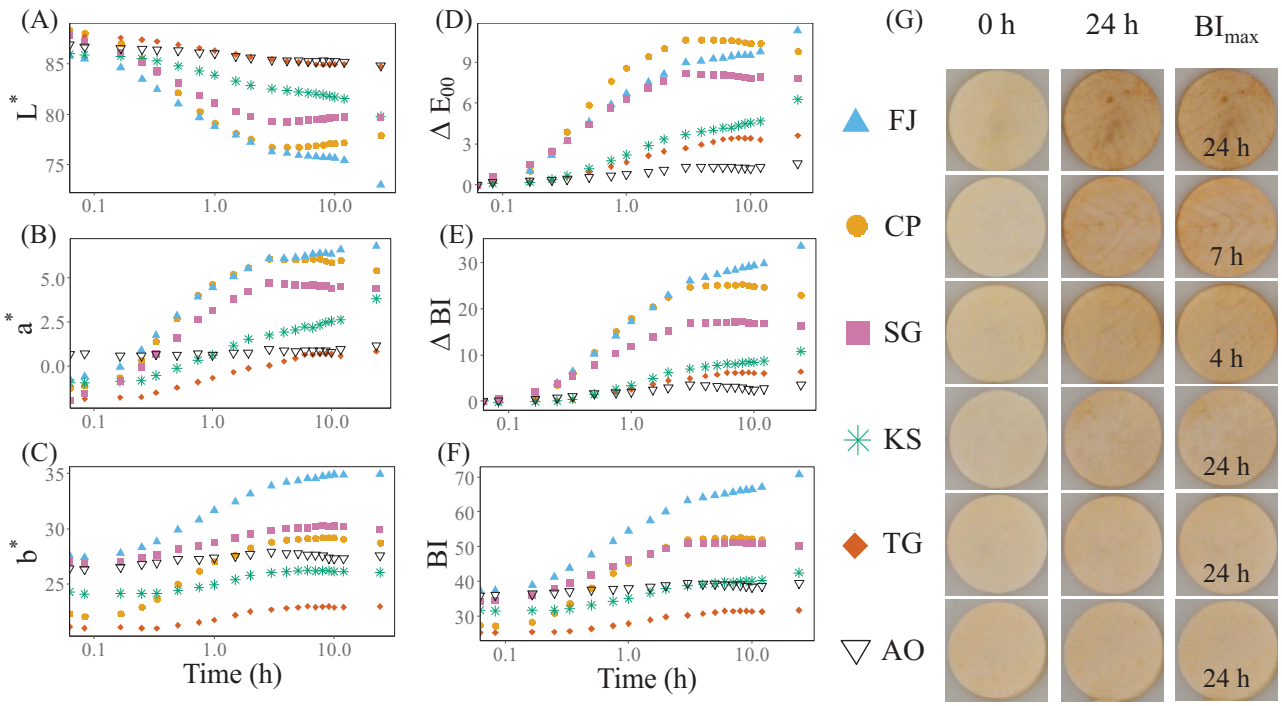

Fig. 3. Time-dependent color change in apple flesh slice samples. The changes in (**A**) L^*, (**B**) a^*, (**C**) b^*, (**D**) ΔE_{00}, (**E**) ΔBI, and (**F**) BI for evaluating the progress of browning in sliced fresh apple samples. L^*, a^*, b^* represent the values on each coordinate axis (lightness, greenness to redness, blueness to yellowness) in the CIE 1976 Laboratory color space. ΔE_{00} is the color difference expressed by the CIE DE 2000 color difference formula. BI is the browning index described in Buera et al. (1985), and ΔBI represents the difference between the two colors. Each marker is presented as the mean value for each of six cultivars: Fuji (FJ), Cripps Pink (CP), Shinanogold (SG), Kinshu (KS), Tsugaru (TG), and Aori27 (AO) (n = 6). (**G**) Images of the apple samples before and after browning. Images in the column BI_{max} were photographed when the maximum BI values were observed. Each sample image was selected by the BI_{max} values that were nearest to the values for each marker.

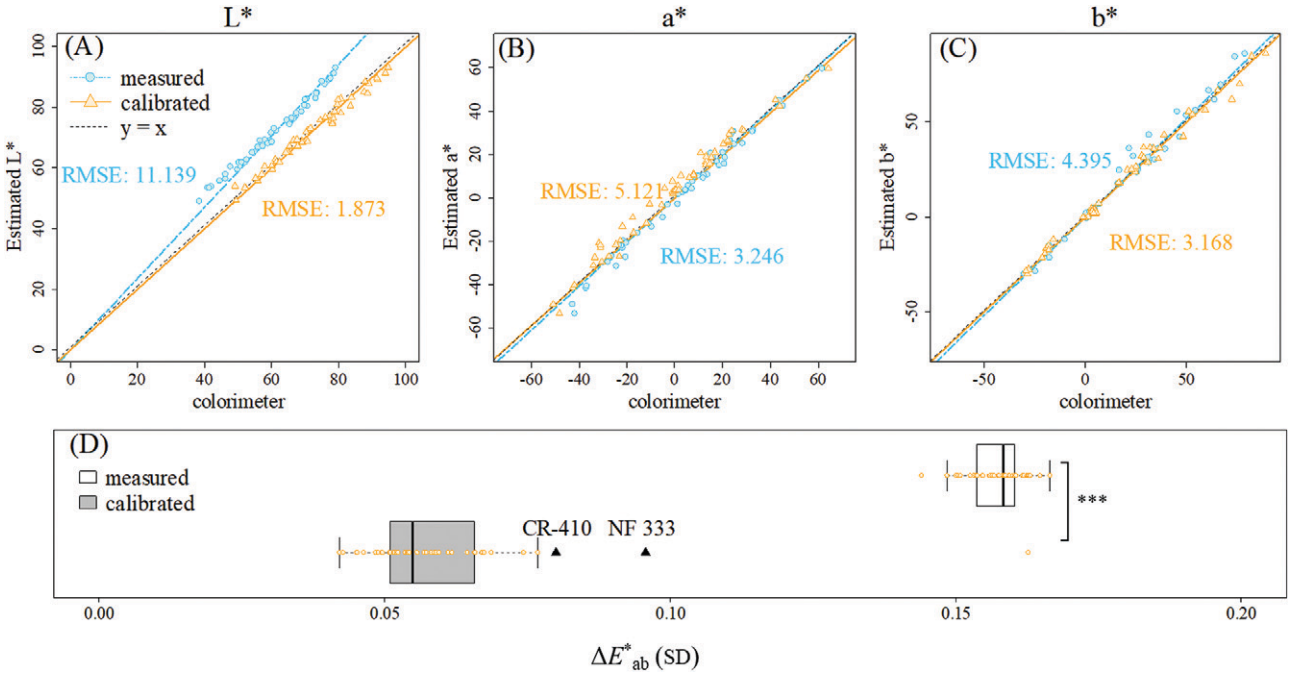

Fig. 4. Accuracy, reproducibility, and interpoint dispersion of the colorimetric system for evaluating apple browning. The (**A**) ***L****, (**B**) ***a****, and (**C**) ***b**** values in the CIE 1976 Laboratory color spaces of 51 selected color standards (different from those used for calibration, Supplemental Table 1) were measured using a colorimeter (NF333; Nippon Denshoku Industries Co., Tokyo, Japan) and estimated using the tested method. Root mean square error (RMSE) was calculated from the values measured by the colorimeter (the y = x lines indicate ideal measurement) and each estimated value. The markers "measured" and "calibrated" indicate the measurement values taken before and after correction using our method. (**D**) Change in measurement dispersion after calibration. The lateral axis indicates the standard deviation (SD) of ΔE^*_{ab}, which represents the degree of the color differences from the mean values of 30 replicate measurements. Orange points indicate the SD of each measured point (n = 42). The triangular markers are the nominal value of a colorimeter (CR-410; Konica Minolta, Tokyo, Japan) colorimeter and the measured value of NF 333. ***Significant differences at $P < 0.001$, as per Student's *t* test.

measurement point located on the edge of the top left side of the imaging region. The interpoint dispersion of the SD, which met the instrumental error of colorimeters, showed that the maximum value of SD in 30 measurements was $\Delta E^*_{ab} = 0.776$. This value was almost the same as the nominal value of $\Delta E^*_{ab} = 0.8$ for the representative sophisticated colorimeter [CR-410 (Table 2)]. The SD of the repeated measurements had a maximum of $\Delta E^*_{ab} = 0.0767$, except for the one previously mentioned point. This was also equivalent to the reproducibility of the nominal value of the CR-410, $\Delta E^*_{ab} = 0.07$ (Fig. 4D).

Changes in the browning indices of reddish-flesh apples. In the slices of reddish-flesh cultivars, the changes in the ***L**** and ***b**** values over time were similar to those of FJ (Fig. 5A and C). The ***a**** values of GN and PP decreased over time, in contrast to the increased values in the FJ samples. However, in the RP and RS samples, the ***a**** values increased after a transient decrease (Fig. 5B). In RP in particular, the value increased after 1.5 h, compared with that at the start of measurement, and a trend different from any other cultivar was confirmed. The ***BI*** values of the reddish-flesh cultivars were higher than those of the other cultivar groups (Fig. 5F), but the ΔBI values before and after browning coincided with the color changes observed in the photographs (Fig. 5E and G). The ΔE_{00} values showed large changes in the FJ samples compared with ΔBI; however, there was no difference between the two indices in the ranking of the values in the reddish-flesh cultivars (Fig. 5D and E).

We then measured the differences in the time courses of the indices, based on the depth of the flesh colors in GN and PP. In the Dr region of the GN samples, a characteristic large maximum change in the ***a**** values ($\Delta a^* = 14.4$) and a slight increase in the ***L**** values were observed over time (Fig. 6B and C). In addition, the ***BI*** values of Dr in GN increased 15 min after processing and then gradually decreased, although the measurement error was larger in this cultivar than in the others tested. In the Pr region of GN, the ΔE_{00}, ΔBI, and change in ***b**** (Δb^*) values were the largest among the four regions measured (Fig. 6D–F). In particular, the Δb^* values had a maximum of 16.3, which was more than twice as large as that in the other regions. In PP, the Δb^* value of Dr was larger than that of Pr, but not in the GN samples. The changes in the six indices of PP were about consistent between the two regions, and the differences in ΔE_{00} and ΔBI were smaller than those for the GN regions.

Changes in browning indices within watercored fruit portions. At the start of measurement, the ***a**** and ***b**** values for the watercored PG samples were higher than those for FJ, while the PG ***L**** values were lower than those for FJ. However, there were few differences in the color change between PG and other yellowish-flesh cultivars during the time course of the measurements (Fig. 5A and B).

The differences in the indices between the Wc and normal portions of the PG samples are shown in Fig. 7. The increase in the ***a**** values of the Wc regions during browning was slow and small, compared with those in the normal portions. Additionally, the ***b**** values of Wc increased, while they decreased in the normal portions of the samples. Before and after browning, the ΔE_{00} values of Wc were about half those of the normal portions, whereas the ΔBI values were more than eight times greater than those of the normal portions.

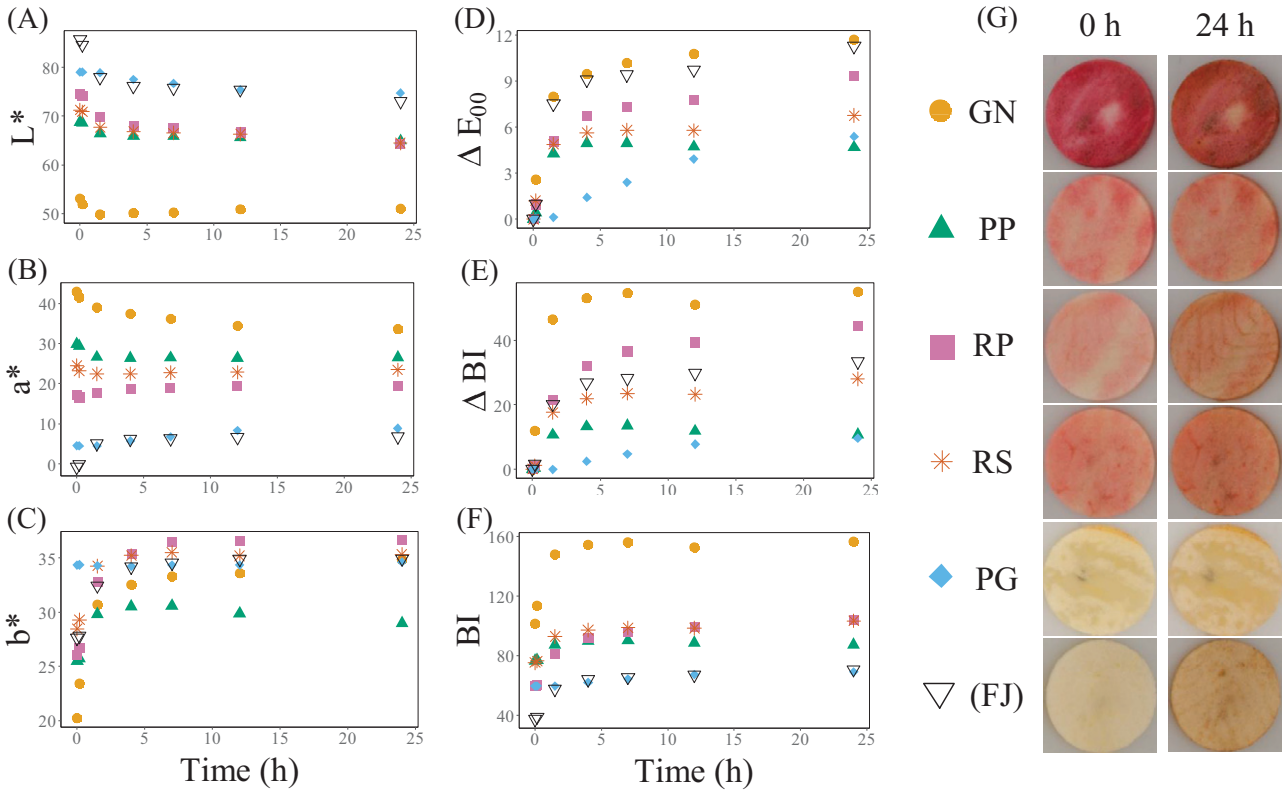

Fig. 5. The time-dependent color changes in the reddish- ['Geneva' (GN), 'Pink Pearl' (PP), 'Rose Pearl' (RP), 'Ruby Sweet' (RS)], watercored- {the hybrid progeny 7-10011 ['Haruka' × 'Aika-no-kaori', (PG)]}, and nomal- ['Fuji'(FJ)]; apple flesh disk samples. The changes in (**A**) L^*, (**B**) a^*, (**C**) b^*, (**D**) ΔE_{00}, (**E**) ΔBI, and (**F**) BI values in reddish-flesh and watercored cultivars during the time course of the experiment (n = 6). L^*, a^*, and b^* represent the values on each coordinate axis (lightness, greenness to redness, blueness to yellowness) in the CIE 1976 Laboratory color space. ΔE_{00} is the color difference expressed by the CIE DE 2000 color difference formula. BI is the browning index described in Buera et al. (1985), and ΔBI represents the difference between the two colors. (**G**) Browning in reddish-flesh and watercored apple samples.

Browning of grated apple samples. The index change of the grated apple samples was very similar to that observed in the sliced samples, but the changes in their browning indices were larger and occurred faster than those in the sliced samples (Figs. 3 and 8; Supplemental Fig. 2). In particular, the greatest changes in the L^* and a^* values were ≈3- to 4-fold larger than those in the sliced samples for FJ (Figs. 3A and 8A); furthermore, the b^* values decreased in grated FJ samples, whereas those of the sliced samples increased. In FJ, TG, and PP, the largest ΔE_{00} values of the grated samples were larger than those measured in the sliced samples, whereas there were few (nonsignificant) differences between the sliced and grated AO, GN, and PG samples. However, the ΔBI values in the grated GN samples were considerably greater than in the other samples (Figs. 3, 5, and 8). The degree of browning roughly corresponded to that of the ranking of the cultivars based on BI values; however, the color of the TG samples 24 h after the start of measurement ($BI \cong 100$) was similar to the color of the PG samples, and did not appear brown (Fig. 8F and G). Altogether, our results show that the measurement accuracy of the color-value extraction method using images is comparable to the nominal values of a sophisticated colorimeter; the degree of apparent browning of the yellow-flesh cultivar flesh disks corresponded to their BI values. The color values and their change tendencies in the browning of the reddish- and watercored-flesh fruit were different from those of normal-flesh cultivars.

Discussion

In this study, we developed a simple and high-throughput system for the quantitative determination of apple flesh browning without using expensive equipment (Figs. 1 and 2). A vegetable slicer and a circular cutting die were used to prepare the flesh disk samples. This eliminated the heterogeneity of shape of samples processed with a knife, and the time required to prepare each sample was reduced to one-tenth of the time required to prepare a grated sample (data not shown). The time elapsed during sample preparation was considered negligible for most apple cultivars, as only one of the eight cultivars showed a visible color change ($\Delta E^*_{ab} \geq 1.0$) within 6 min after sample preparation (Supplemental Fig. 3A), which was the average time required to prepare 42 samples. These results indicate that flesh disks are suitable samples for efficient evaluation of flesh browning.

In addition, we attempted to eliminate image color-value deviations owing to the influence of optical conditions only using correction based on inexpensive color standards rather than a colorimeter. The indirect illumination, made with reference to Yamamoto et al. (2011), allowed a uniform light environment, such as that achieved by a colorimeter (Supplemental Fig. 1). The calibration by the SSANOVA regression model and the background correction reduced the deviation of the L^* and b^* values observed with colorimetry measurements. In our method, the SD of ΔE^*_{ab} based on measurement position and the SD based on measurement replication were equivalent to the nominal

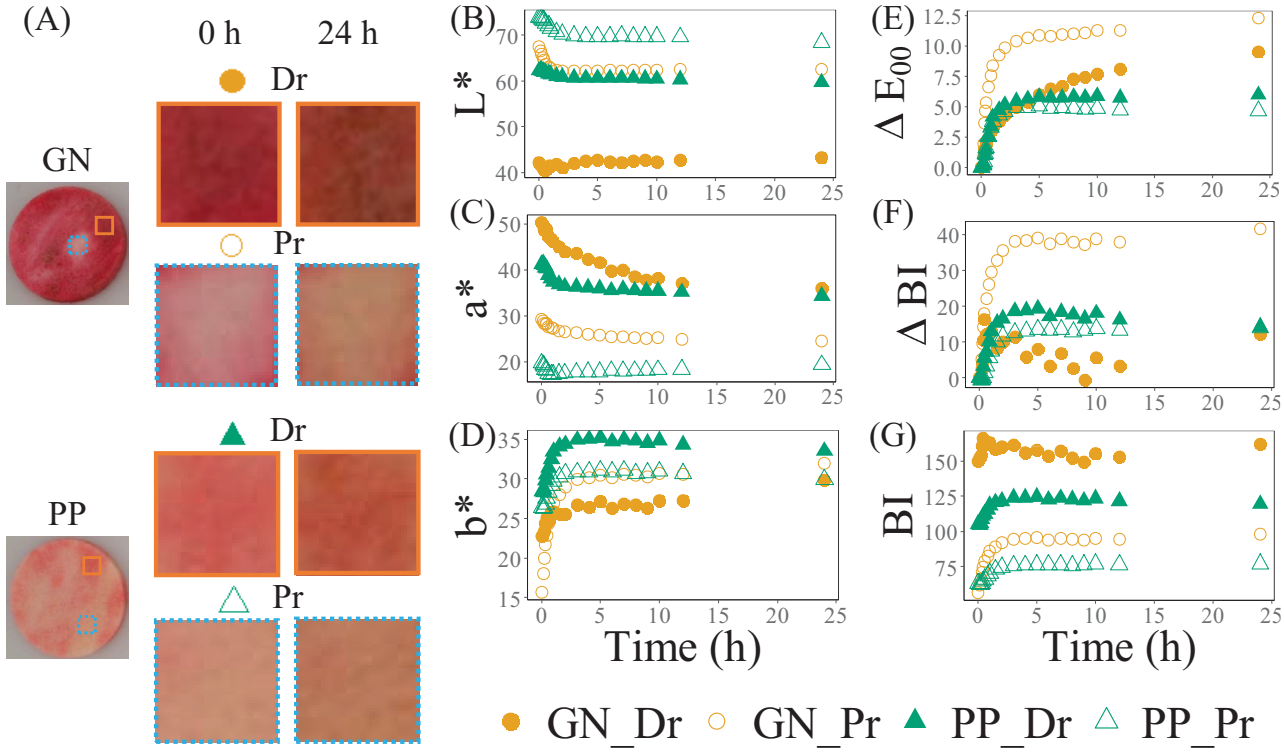

Fig. 6. Changes of the colorimetric values of browning in deep red (Dr)- and pale red (Pr)-colored apple flesh. (**A**) The assigned Dr/Pr regions in cultivars Geneva (GN) and Pink Pearl (PP). The changes in the (**B**) L^*, (**C**) a^*, (**D**) b^*, (**E**) ΔE_{00}, (**F**) ΔBI, and (**G**) BI values in the four portions during the time course of the experiment (n = 3). L^*, a^*, and b^* represent the values on each coordinate axis (lightness, greenness to redness, blueness to yellowness) in the CIE 1976 Laboratory color space. ΔE_{00} is the color difference expressed by the CIE DE 2000 color difference formula. BI is the browning index described in Buera et al. (1985), and ΔBI represents the difference between the two colors.

values of a commercial sophisticated colorimeter. However, there is still room for improving the measurement accuracy of this method. For example, in the upper left corner of the image, the SD of the ΔE^*_{ab} value during measurement replication was larger than that before calibration (Fig. 4D). This difference in the magnitude of the dispersion of each measurement point might arise from the difference in the amount of light received at the center of the image and at the periphery, owing to the use of a wide-angle lens. This problem may be solved by examining the dispersion of each measurement point in advance and removing points with insufficient repeatability, or by adding reference ROIs such that the calculation load is not excessively increased.

In addition to its high throughput, high accuracy, and low labor costs, our method demonstrates three other advantages of using digital camera images to obtain color values. The first is that browning is recorded as an image; thus, the numerical value can be compared with the degree of browning appearance. Compared with methods using a colorimeter, in which only numerical data are recorded, in our method, it is easy to specify the cause of the difference when an outlier is observed, because the image of the sample corresponding to the measured value is always available. Hence, the risk of wasting all the experimental data at one time is considerably reduced. Second, our method achieves smaller human error, as the sample colors are measured from a remote location; therefore, the risk of contamination of the samples is limited and stable results are reliably obtained by averaging a wide range of measurements of each sample. The third advantage is that the positional relationship between samples is fixed during measurement, which limits the risk of mixing the data between cultivars and fruit. Evaluating apple flesh browning using our system can greatly reduce the failure of an experiment owing to operation error, especially when processing large numbers of experimental samples. Thus, our method provides a more stable measurement platform, compared with conventional colorimetric methods.

As described previously, our method can simultaneously measure a plurality of samples with little human error, although it is inferior to a colorimeter in ease of use and more expensive than an inexpensive device, such as the Nix Pro 2 (Table 2). These features make this method suitable for experiments with large sample sizes and time-course measurements. In addition, this method facilitates site-specific analysis, as shown in Figs. 6 and 7. This is because the measuring position and measuring range can be freely set.

We also analyzed the changes in color values owing to the browning of apple flesh by measuring flesh disks over time, using our newly developed method (Figs. 3 and 5). The size of the BI values used as an indicator of browning and the color tone of each sample were in good agreement, unless the values of the grated GN samples were unstable, similar to the measurements in the Dr region of the flesh disks (Figs. 5F and 8F). This indicates that it is possible to quantitatively evaluate the degree of browning using the BI values of normal (yellow or white) apple flesh colors (Fig. 3). Because the b^* value is included in the calculation formula of BI, it is a more appropriate evaluation of apple color tone.

In the samples from the reddish-flesh cultivars, the BI values were generally higher than those of the other cultivars (Figs. 3F and 5F). In addition, the measured BI values of the grated GN samples were unstable, similar to the measurements in the Dr region of the flesh disks (Figs. 5F and 8F). Since their L^* and a^*

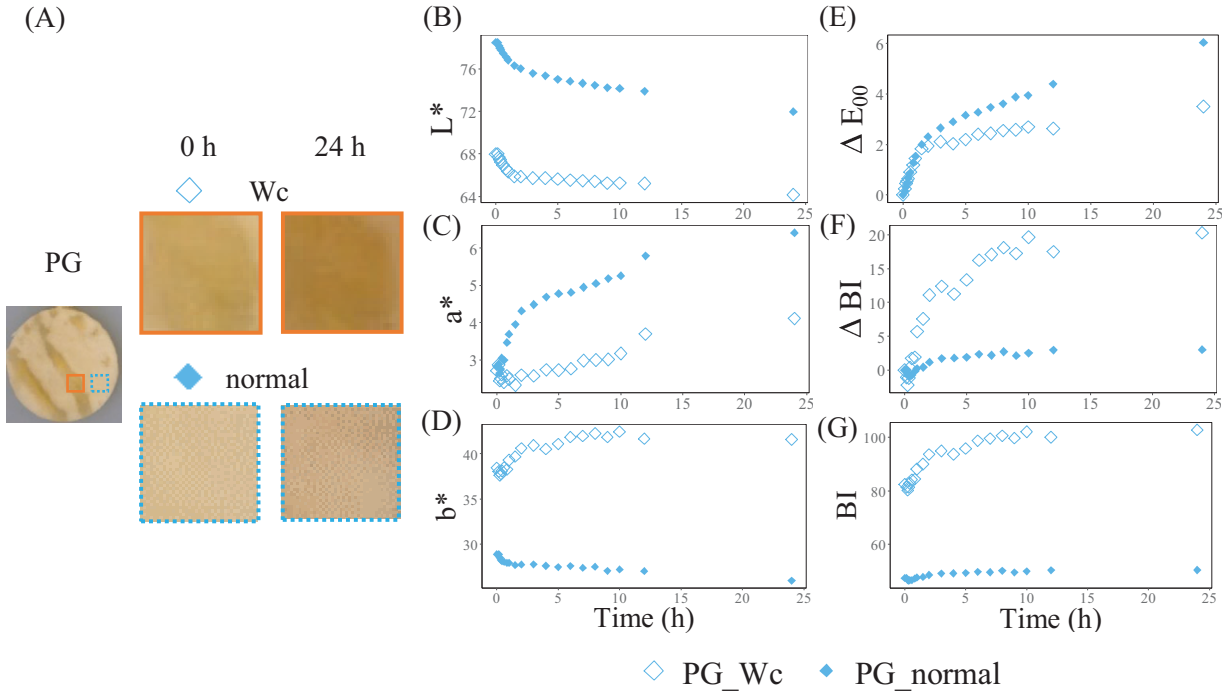

Fig. 7. Changes in the browning colorimetric values in watercored portions of apple flesh. (**A**) The portions assigned as the watercored (Wc) and normal areas of the hybrid progeny 7-10011 ['Haruka' × 'Aika-no-kaori', (PG)]. The time-course changes in (**B**) ***L****, (**C**) ***a****, (**D**) ***b****, (**E**) ΔE_{00}, (**F**) ΔBI, and (**G**) ***BI*** values in the two portions (n = 3). ***L****, ***a****, and ***b**** represent the values on each coordinate axis (lightness, greenness to redness, blueness to yellowness) in the CIE 1976 Laboratory color space. ΔE_{00} is the color difference expressed by the CIE DE 2000 color difference formula. ***BI*** is the browning index described in Buera et al. (1985), and ΔBI represents the difference between the two colors.

values were significantly different from those of the yellowish cultivars, there is a risk in treating the ***BI*** values of the reddish-flesh cultivars the same as those of yellowish-flesh cultivars, especially as an absolute browning degree indicator. In addition, the ***BI*** values varied with the depth of the red color of the apple sample (Figs. 6G and 8F).

The ΔE_{00} and ΔBI values before and after browning were calculated as indices that indicate the degree of coloration change of the cut surface of the flesh disk, and the correspondence between these indices and the visually evaluated color differences were confirmed (Fig. 3D, E, and G).

From the observations of the changes in ΔE_{00} and ΔBI over time, we show that cultivars can be classified into two groups (Fig. 3): cultivars with ΔE_{00} and ΔBI values that increased between 12 and 24 h after sample processing (FJ, KS, TG, and AO) and cultivars whose ΔE_{00} and ΔBI values decreased during this time interval (CP and SG). These results suggest that the changes in flesh disk coloration rate over time are caused not only by the chemical equilibrium in a single enzymatic reaction, but by multiple factors. In this experiment, both ΔE_{00} and ΔBI reflected the degree of coloration well, but the magnitude of the correlation between FJ and CP 24 h after the start of measurement was opposite in ΔE_{00} ΔBI. The intercultivar differences in ΔBI agreed more with those observed through visual perception, suggesting that ΔE_{00} should not be used in the measurement of cultivars that show a large degree of browning. ΔE_{00} indicates an improved index representing color differences that approximate human vision, and the values were adjusted to the visual experience, such that the deeper the color, the lower the color difference perception (Luo et al., 2001). Considering this adjustment, the ΔE_{00} of a yellowish-flesh sample with higher color saturation could be calculated to be much smaller than that of the sensory difference.

The relationship between ΔE_{00} and ΔBI in the reddish-flesh cultivars was similar to that in the yellowish-flesh samples; ΔE_{00} was relatively smaller than ΔBI in the samples with relatively bright colors (Fig. 5D, E, and G). Therefore, although the degree of color change can be quantified using both ΔE_{00} and ΔBI, as in the yellowish cultivars, it is necessary to examine the index used for evaluating the color tone in reddish-flesh cultivars in future analyses.

The results for the change in the color values of watercored PG samples over time showed that the color change in the PG samples was similar to that of normal yellowish-flesh cultivars, and that it was possible to determine the degree of browning using either index (Fig. 5). However, the ***L****, ***a****, and ***b**** values of the Wc portions, and their changes, were different from those in normal-flesh portions (Fig. 7). Because the watercored area was translucent, its color changes depended on the background, and because gray was used as the background color in our method, the watercored samples were artificially made to look as if they were browning. Therefore, the correction effect of ΔE_{00} had a greater influence on these results than in the normal-flesh samples. The colorimetry of translucent materials is usually performed by measuring spectral transmittance, not by directly reading the tristimulus value, which was simulated in our method. Therefore, the estimation method used must be reevaluated to accurately measure browning from images of watercored apple samples.

In the grated samples, the trends in the ΔE_{00} and ΔBI values were not much different from those of the sliced samples, and the difference appeared to be only a greater extent of change. However, with their lower ***L**** and ***b**** values and higher ***a**** values, the

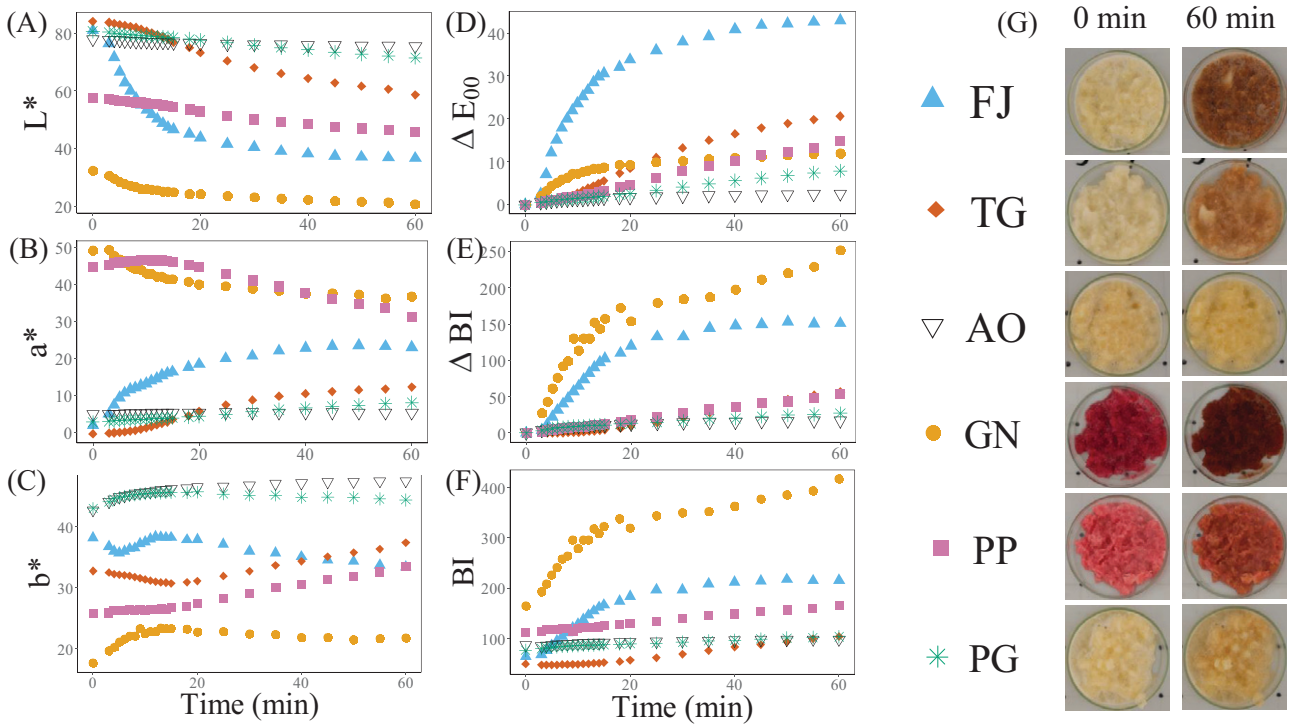

Fig. 8. Time-series measurements of grated apple flesh samples. The time-course changes in (**A**) ***L****, (**B**) ***a****, (**C**) ***b****, (**D**) ΔE_{00}, (**E**) ΔBI, and (**F**) ***BI*** values from grated samples of five apple cultivars [Fuji (FJ), Tsugaru (TG), Aori27 (AO), Geneva (GN), and Pink Pearl (PP)] and one hybrid progeny 7-10011 ['Haruka' × 'Aika-no-kaori', (PG)] (n = 3). ***L****, ***a****, and ***b**** represent the values on each coordinate axis (lightness, greenness to redness, blueness to yellowness) in the CIE 1976 Laboratory color space. ΔE_{00} is the color difference expressed by the CIE DE 2000 color difference formula. ***BI*** is the browning index described in Buera et al. (1985), and ΔBI represents the difference between the two colors. (**G**) Images were taken before and 60 min after sample processing.

accuracy of the quantification of the degree of browning using ***BI*** may not be as accurate. When a dark reddish-purple color, such as that of GN, was expressed as RGB luminance, the ***G*** and ***B*** values were very small [0–30 (Fig. 8G, Supplemental Fig. 4)]. These values may have been outside the dynamic range of the image sensor, or the calibration range of the ***R***, ***G***, and ***B*** values may have been insufficient for successful sample measurement. These results might be improved by using a camera capable of obtaining more gradation-rich images or by using more standard color samples for calibration, with ***G*** and ***B*** values that are close to zero.

In the Dr portion of GN, the Wc portion of PG, and the grated samples of FJ, TG, GN, and PP, the value of ΔE_{00} did not match the magnitude of the coloration observed from the image (Figs. 6A and E, 7A and E, and 8D and G). These flesh types are all characterized by a particularly deep color after coloration. Therefore, it is presumed that even in these cases, the correction included in the ΔE_{00} calculation formula is too strong.

5The suitability of the indices used in this study for the quantitative evaluation of apple browning is summarized in Table 3. Both ΔE_{00} and ***BI*** corresponded to more diverse samples than ***L****, ***a****, ***b****, and ***BI*** was particularly suitable for evaluating normal yellowish flesh. However, ΔE_{00} may not be consistent with visual perception for deep colors, and ***BI*** was limited when measuring dark-reddish-purple flesh and watercored areas.

In conclusion, we have developed a system for quantifying apple flesh browning. The system can reduce human measurement errors while achieving high efficiency at the same level of color measurement performance as a sophisticated colorimeter, by using a digital camera and standardized apple flesh disk samples. ***BI*** was useful as an index to quantify the degree of browning and

Table 3. The ability of each index to evaluate degree of apple flesh browning. "Excellent" is the best indicator. "Good" is a generally good indicator, but depending on the conditions, browning cannot always be expressed well. "Poor" indicates that the evaluation of browning is difficult.

Sample	Color descriptor[z]	***L**** (Δ***L****)	***a**** (Δ***a****)	***b****(Δ***b****)	ΔE_{00}	***BI***	ΔBI
Normal flesh	Depth of brown	Good	Good	Poor	–	Excellent	–
	Degree of discoloration	Good	Good	Poor	Good	–	Excellent
Reddish flesh	Depth of brown	Poor	Poor	Poor	–	Good	–
	Degree of discoloration	Poor	Poor	Poor	Good	–	Good
Watercored flesh	Depth of brown	Poor	Poor	Poor	–	Poor	–
	Degree of discoloration	Good	Poor	Poor	Good	–	Good

[z]***L****, ***a****, and ***b**** represent the values on each coordinate axis (lightness, greenness to redness, blueness to yellowness) in the CIE 1976 Laboratory color space, and Δ***L****, Δ***a****, and Δ***b****are the difference between the two colors. ΔE_{00} is the color difference expressed by the CIE DE 2000 color difference formula. ***BI*** is the browning index described in Buera et al. (1985), and ΔBI represents the difference between the two colors.

it was possible to observe this index changing over time to evaluate the progress of browning. However, there may be different patterns of browning in reddish and watercored flesh, suggesting that different kinds of apple flesh should not be evaluated using the same conditional parameters. This method can be further improved to more accurately measure the color values of dark reddish-purple apple flesh, and it will be necessary to devise ways to expand the dynamic range of the color measurement and develop an index that can accurately express the color change of reddish-flesh apples as browning proceeds.

Literature Cited

Amiot, M.J., M. Tacchini, S.Y. Aubert, and W. Oleszek. 1995. Influence of cultivar, maturity stage, and storage conditions on phenolic composition and enzymic browning of pear fruits. J. Agr. Food Chem. 43:1132–1137, doi: 10.1021/jf00053a004.

Arakawa, O. and S. Komori. 2006. Apple, p. 34–42. In: Jpn. Soc. Hort. Sci. (ed.). Horticulture in Japan. Shoukadoh Publ., Kyoto, Japan.

Bennedsen, B.S. and D.L. Peterson. 2005. An optical method for detecting watercore and mealiness in apples. Trans. ASAE 48:1819–1826, doi: 10.13031/2013.19979.

Buera, M.P., R.D. Lozano, and C. Petriella. 1985. Definition of color in the non-enzymatic browning process. Farbe 32/33:316–326.

Cabezas-Serrano, A.B., M.L. Amodio, R. Cornacchia, R. Rinaldi, and G. Colelli. 2009. Screening quality and browning susceptibility of five artichoke cultivars for fresh-cut processing. J. Sci. Food Agr. 89: 2588–2594, doi: 10.1002/jsfa.3759.

Carter, N. 2012. Petition for determination of nonregulated status: Arctic™ apple (*Malus* × *domestica*) events GD743 and GS784. U.S. Dept. Agr., Animal Plant Health Inspection Serv., Riverdale, MD.

Coseteng, M.Y. and C.Y. Lee. 1987. Changes in apple polyphenoloxidase and polyphenol concentrations in relation to degree of browning. J. Food Sci. 52:985–989, doi: 10.1111/j.1365-2621.1987.tb14257.x.

Guardo, M.D., A. Tadiello, B. Farneti, G. Lorenz, D. Masuero, U. Vrhovsek, G. Costa, R. Velasco, and F. Costa. 2013. A multidisciplinary approach providing new insight into fruit flesh browning physiology in apple (*Malus* × *domestica* Borkh.). PLoS One 8:e78004, doi: 10.1371/journal.pone.0078004.

Hodgen, J. 2016. Comparison of nix color sensor and Nix Color Sensor Pro to standard meat science research colorimeters. Meat Sci. 112: 159, doi: 10.1016/j.meatsci.2015.08.129.

Holman, B.W.B., D. Collins, A.K. Kilgannon, and D.L. Hopkins. 2018. The effect of technical replicate (repeats) on Nix Pro Color Sensor™ measurement precision for meat: A case-study on aged beef colour stability. Meat Sci. 135:42–45, doi: 10.1016/j.meatsci.2017.09.001.

Hunt, R.W.G. and M.R. Pointer. 2011. Measuring colour. 4th ed. Wiley, Chichester, UK, doi: 10.1002/9781119975595.

Igarashi, M., Y. Hatsuyama, T. Harada, and T. Fukasawa-Akada. 2016. Biotechnology and apple breeding in Japan. Breed. Sci. 66: 18–33, doi: 10.1270/jsbbs.66.18.

Lee, C.Y., V. Kagan, A.W. Jaworski, and S.K. Brown. 1990. Enzymic browning in relation to phenolic compounds and polyphenoloxidase activity among various peach cultivars. J. Agr. Food Chem. 38: 99–101, doi: 10.1021/jf00091a019.

León, K., D. Mery, F. Pedreschi, and J. León. 2006. Color measurement in $L^*a^*b^*$ units from RGB digital images. Food Res. Int. 39: 1084–1091, doi: 10.1016/j.foodres.2006.03.006.

Lu, S., Y. Luo, E. Turner, and H. Feng. 2007. Efficacy of sodium chlorite as an inhibitor of enzymatic browning in apple slices. Food Chem. 104:824–829, doi: 10.1016/j.foodchem.2006.12.050.

Lunadei, L., P. Galleguillos, B. Diezma, L. Lleó García, and L. Ruiz-Garcia. 2011. A multispectral vision system to evaluate enzymatic browning in fresh-cut apple slices. Postharvest Biol. Technol. 60:225–234, doi: 10.1016/j.postharvbio.2011.02.001.

Lunadei, L., P. Galleguillos, B. Diezma Iglesias, and L. Lleó García. 2010. Evaluation of enzymatic browning in fresh-cut apple slices applying a multispectral vision system. Proc. Intl. Conf. Agr. Eng., AgEng 2010. Towards environmental technologies. EUIT Agrícola (UPM), Clermont-Ferrand, France.

Luo, M.R., G. Cui, and B. Rigg. 2001. The development of the CIE 2000 colour-difference formula: CIEDE2000. Color Res. Appl. 26: 340–350, doi: 10.1002/col.1049.

Lv, B., B. Li, S. Chen, J. Chen, and B. Zhu. 2009. Comparison of color techniques to measure the color of parboiled rice. J. Cereal Sci. 50:262–265, doi: 10.1016/j.jcs.2009.06.004.

Murata, M., M. Tsurutani, M. Tomita, S. Homma, and K. Kaneko. 1995. Relationship between apple ripening and browning: Changes in polyphenol content and polyphenol oxidase. J. Agr. Food Chem. 43:1115–1121, doi: 10.1021/jf00053a001.

Oliveira, M., M. Abadias, J. Usall, R. Torres, N. Teixidó, and I. Viñas. 2015. Application of modified atmosphere packaging as a safety approach to fresh-cut fruits and vegetables—A review. Trends Food Sci. Technol. 46:13–26, doi: 10.1016/j.tifs.2015.07.017.

Pristijono, P., R.B.H. Wills, and J.B. Golding. 2006. Inhibition of browning on the surface of apple slices by short term exposure to nitric oxide (NO) gas. Postharvest Biol. Technol. 42:256–259, doi: 10.1016/j.postharvbio.2006.07.006.

Prohens, J., A. Rodríguez-Burruezo, M.D. Raigón, and F. Nuez. 2007. Total phenolic concentration and browning susceptibility in a collection of different varietal types and hybrids of eggplant: Implications for breeding for higher nutritional quality and reduced browning. J. Amer. Soc. Hort. Sci. 132:638–646, doi: 10.21273/jashs.132.5.638.

Quevedo, R., M. Jaramillo, O. Díaz, F. Pedreschi, and J.M. Aguilera. 2009. Quantification of enzymatic browning in apple slices applying the fractal texture Fourier image. J. Food Eng. 95:285–290, doi: 10.1016/j.jfoodeng.2009.05.007.

Quevedo, R., E. Valencia, P. López, E. Gunckel, F. Pedreschi, and J. Bastías. 2014. Characterizing the variability of enzymatic browning in fresh-cut apple slices. Food Bioprocess Technol. 7:1526–1532, doi: 10.1007/s11947-013-1226-1.

Quevedo, R., F. Pedreschi, J.M. Bastías, and O. Díaz. 2016. Correlation of the fractal enzymatic browning rate with the temperature in mushroom, pear, and apple slices. Lebensm. Wiss. Technol. 65:406–413, doi: 10.1016/j.lwt.2015.08.052.

Robertson, A.R. 1977. The CIE 1976 color-difference formulae. Color Res. Appl. 2:7–11, doi: 10.1002/j.1520-6378.1977.tb00104.x.

Stiglitz, R., E. Mikhailova, C. Post, M. Schlautman, and J. Sharp. 2016. Evaluation of an inexpensive sensor to measure soil color. Comput. Electron. Agr. 121:141–148, doi: 10.1016/j.compag.2015.11.014.

International Electrotechnical Commission. 1999. Multimedia systems and equipment-colour measurement and management-part 2-1: Colour management-default RGB colour space-sRGB. Intl. Electrotechnical Commission 61966-2-1.

Tazawa, J., H. Oshino, T. Kon, S. Kasai, T. Kudo, Y. Hatsuyama, T. Fukasawa-Akada, T. Yamamoto, and M. Kunihisa. 2019. Genetic characterization of flesh browning trait in apple using the non-browning cultivar 'Aori 27.' Tree Genet. Genomes 15:49, doi: 10.1007/s11295-019-1356-3.

Veltman, R.H., C. Larrigaudiere, H.J. Wichers, A.C.R. van Schaik, L.H.W. van der Plas, and J. Oosterhaven. 1999. PPO Activity and polyphenol content are not limiting factors during brown core development in pears (*Pyrus communis* L. cv. Conference). J. Plant Physiol. 154:697–702, doi: 10.1016/S0176-1617(99)80247-8.

Yam, K.L. and S.E. Papadakis. 2004. A simple digital imaging method for measuring and analyzing color of food surfaces. J. Food Eng. 61: 137–142, doi: 10.1016/S0260-8774(03)00195-X.

Yamamoto, K., Y. Kimura, T. Togami, Y. Yoshioka, A. Hashimoto, and T. Kameoka. 2011. A chromatic image analysis system using content-based image retrieval. Agr. Inf. Res. (NogyoJyohokenkyu). 20:139–147 (In Japanese), doi: 0.3173/air.20.139.

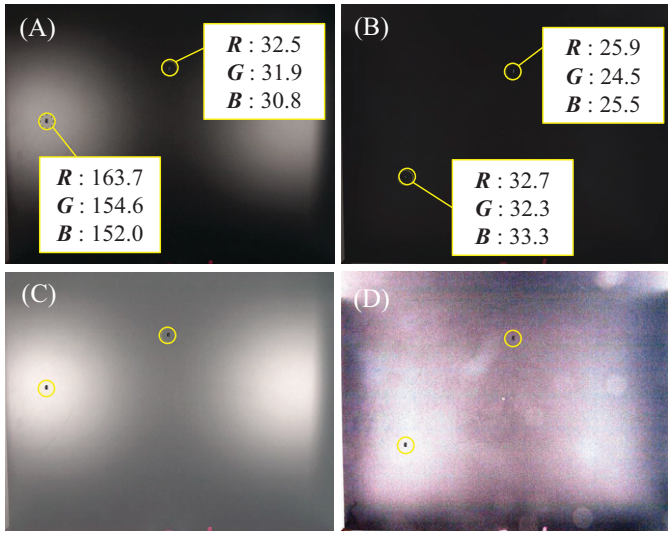

Supplemental Fig. 1. The unevenness in brightness of photographic ranges depending on lighting conditions. (**A**) When the light source was arranged above the area to photograph, or (**B**) when a light reflector was used. The numbers yellow frames are red (*R*), green (*G*), and blue (*B*) intensity values in the lighter and darker areas (yellow circles). (**C**) and (**D**) show the images in (**A**) and (**B**) after contrast regulation.

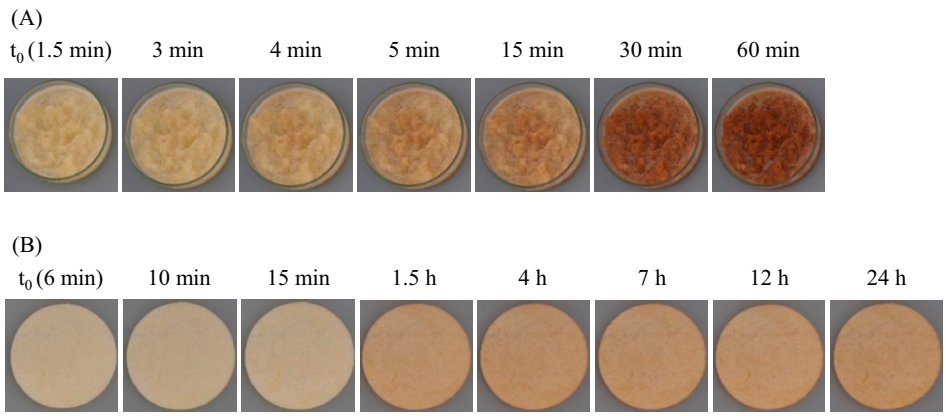

Supplemental Fig. 2. Images of time-course color changes of the apple 'Fuji' flesh samples. (**A**) The grated sample. (**B**) The sliced sample.

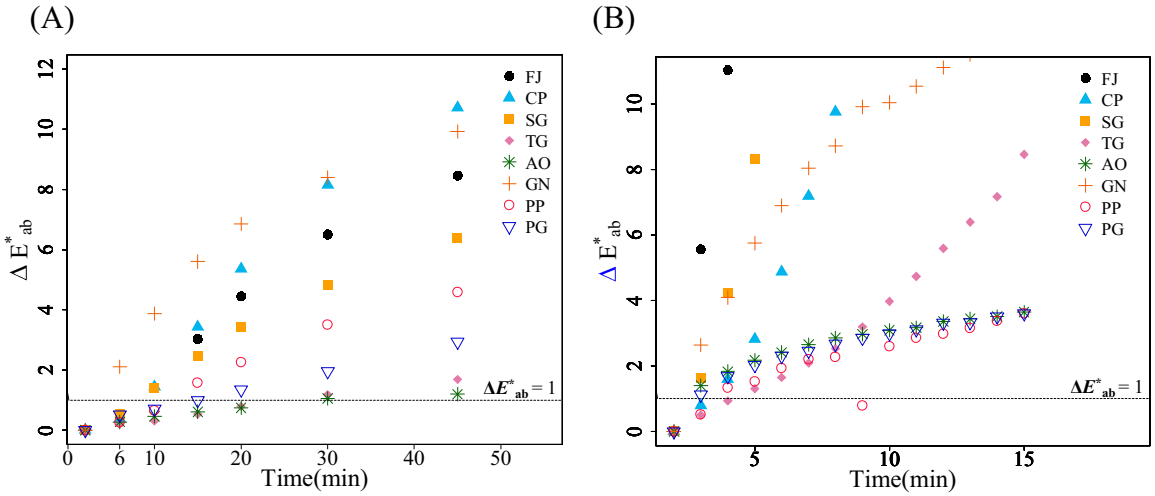

Supplemental Fig. 3. The temporal changes in the color difference values (ΔE^*_{ab}) of seven apple cultivars [Fuji (FJ), Cripps Pink (CP), Shinano Gold (SG), Tsugaru (TG), Aori27 (AO), Geneva (GN), and Pink Pearl (PP)] and one hybrid progeny '7-10011' (PG) immediately after sample processing (n = 3). (**A**) The color changes of the sliced flesh samples. (**B**) The color changes of the grated flesh samples. Dotted lines of both figures indicate $\Delta E^*_{ab}=1$, which is a value often used as a criterion for human perception of color differences.

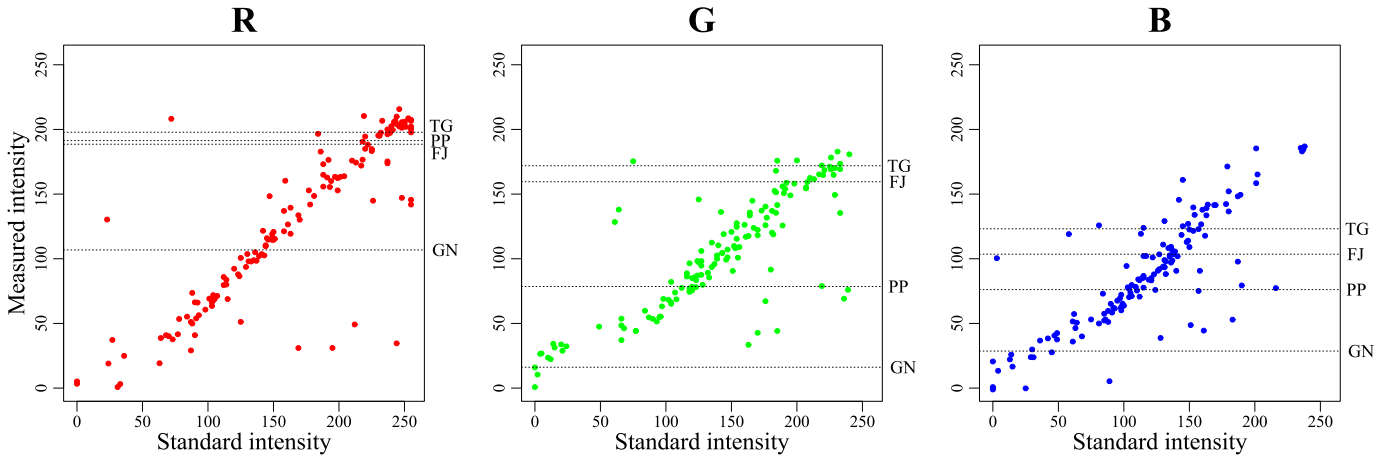

Supplemental Fig. 4. Measured red (*R*), green (*G*), and blue (*B*) intensity of the color standards (Pantone Formula Guide Solid Coated & Uncoated; Pantone LLC, Carlstadt, NJ) and the grated apple-flesh samples. Each marker represents 140 samples of the color standard used for calibration. The vertical axis represents the measured values before calibration, and the horizontal axis represents the standard values which are used in the calibration. The dotted lines show the measurement values immediately after processing of the samples of grated flesh of four cultivars [Fuji (FJ), Tsugaru (TG), Geneva (GN), and Pink Pearl (PP)].

Supplemental Table 1. Color standard samples used to calibrate the intensities of Red (R), Green (G), and Blue (B). The samples presented with a gray background were only used for the accuracy test.

Sample	R	G	B
PANTONE®127U	244	228	131
PANTONE®128U	243	207	95
PANTONE®129U	242	176	61
PANTONE®130U	240	155	45
PANTONE®131U	181	128	49
PANTONE®132U	146	120	49
PANTONE®182U	255	183	202
PANTONE®183U	255	140	163
PANTONE®184U	248	107	131
PANTONE®226U	218	66	136
PANTONE®233U	199	68	136
PANTONE®278U	151	184	237
PANTONE®283U	163	198	238
PANTONE®291U	139	189	235
PANTONE®382U	142	195	25
PANTONE®389U	177	221	0
PANTONE®420U	188	190	189
PANTONE®421U	178	181	180
PANTONE®422U	158	161	162
PANTONE®423U	144	147	150
PANTONE®424U	135	137	137
PANTONE®425U	123	124	126
PANTONE®426U	104	98	104
PANTONE®1767U	255	185	201
PANTONE®1777U	255	125	145
PANTONE®1787U	248	127	113
PANTONE®2001U	250	236	158
PANTONE®2002U	251	233	131
PANTONE®2003U	250	233	115
PANTONE®2004U	253	226	115
PANTONE®2005U	255	220	130
PANTONE®2006U	233	192	102
PANTONE®2040U	218	64	106
PANTONE®2092U	188	170	216
PANTONE®2162U	158	164	179
PANTONE®2163U	145	160	178
PANTONE®2164U	136	150	169
PANTONE®2165U	120	135	154
PANTONE®2166U	112	125	144
PANTONE®2167U	105	116	137
PANTONE®2168U	90	104	117
PANTONE®2218U	125	176	190
PANTONE®2219U	112	164	180
PANTONE®2220U	104	154	170
PANTONE®2221U	92	144	160
PANTONE®2223U	78	127	145
PANTONE®2224U	68	116	134
PANTONE®2260U	195	219	187
PANTONE®2261U	147	184	142
PANTONE®2262U	143	173	141
PANTONE®2263U	125	154	122
PANTONE®2264U	114	152	111
PANTONE®2265U	115	143	112
PANTONE®2266U	88	118	84
PANTONE®2281U	212	239	151
PANTONE®2282U	192	240	149
PANTONE®2283U	159	231	115
PANTONE®2420U	23	200	114
PANTONE®2437U	244	191	157
PANTONE®2444U	220	166	157
PANTONE®3514U	237	181	58
PANTONE®3517U	184	61	68
PANTONE®3519U	226	163	161
PANTONE®3544U	225	182	159
PANTONE®3547U	186	142	81
PANTONE®3588U	255	151	75
PANTONE®3596U	219	180	128
PANTONE®3599U	213	189	127
PANTONE®3965U	237	233	3
PANTONE®5395U	72	75	89
PANTONE®5463U	64	77	85
PANTONE®5517U	169	185	183
PANTONE®7401U	248	229	164
PANTONE®7402U	237	219	153
PANTONE®7403U	237	207	127
PANTONE®7404U	244	208	62
PANTONE®7405U	222	177	4
PANTONE®7406U	232	185	36
PANTONE®7407U	199	163	109
PANTONE®7457U	194	226	236
PANTONE®7482U	27	167	110
PANTONE®7730U	101	156	121
PANTONE®7731U	84	146	106
PANTONE®7732U	70	133	98
PANTONE®7733U	73	123	98
PANTONE®7734U	87	118	100
PANTONE®7735U	93	108	98
PANTONE®7736U	91	104	98
PANTONE®Warm Gray 6U	161	154	149
PANTONE®Warm Gray 7U	149	143	138
PANTONE®Warm Gray 8U	141	135	131
PANTONE®Warm Gray 9U	133	127	123
PANTONE®Warm Gray 10U	129	123	119
PANTONE®Warm Gray 11U	124	118	115
PANTONE®Black 2U	98	96	81
PANTONE®Black 3U	88	93	88
PANTONE®Black 4U	103	95	85
PANTONE®Black 5U	103	90	91
PANTONE®Black 6U	77	77	86
PANTONE®Black 7U	107	104	99
PANTONE®103C	188	170	0
PANTONE®109C	246	210	0
PANTONE®112C	150	132	14
PANTONE®1245C	191	147	15
PANTONE®126C	149	118	13
PANTONE®176C	255	176	187
PANTONE®177C	255	127	139
PANTONE®178C	253	87	93
PANTONE®186C	197	12	47
PANTONE®2001C	241	229	153
PANTONE®2022C	246	170	140
PANTONE®2035C	210	0	29

(Continued on next page)

Supplemental Table 1. Continued.

Sample	R	G	B
PANTONE®213C	225	20	121
PANTONE®214C	204	4	105
PANTONE®215C	170	15	90
PANTONE®219C	217	14	132
PANTONE®227C	169	0	98
PANTONE®228C	137	5	88
PANTONE®2347C	220	2	0
PANTONE®2411C	24	66	31
PANTONE®3542C	63	10	124
PANTONE®3583C	90	24	132
PANTONE®408C	150	139	135
PANTONE®409C	131	120	115
PANTONE®410C	114	102	97
PANTONE®660C	87	124	201
PANTONE®661C	31	49	148
PANTONE®662C	33	21	112
PANTONE®7401C	239	225	163
PANTONE®7402C	230	217	150
PANTONE®7403C	231	213	130
PANTONE®7502C	201	184	135
PANTONE®7503C	163	153	103
PANTONE®7504C	144	120	92
PANTONE®7515C	193	139	104
PANTONE®7516C	149	84	42
PANTONE®7517C	130	66	30
PANTONE®7732C	0	122	61
PANTONE®7733C	0	112	64
PANTONE®7734C	36	97	63
PANTONE®Yellow U	255	225	0
PANTONE®Yellow 0131U	243	246	153
PANTONE®169U	255	183	174
PANTONE®170U	255	140	125
PANTONE®171U	255	119	100
PANTONE®172U	254	102	77
PANTONE®173U	202	97	74
PANTONE®Red 0331U	255	176	190
PANTONE®406U	198	190	185
PANTONE®407U	170	162	159
PANTONE®408U	156	148	147
PANTONE®409U	147	139	137
PANTONE®410U	137	129	127
PANTONE®Magenta 0521U	249	168	220
PANTONE®Violet 0631U	192	145	223
PANTONE®Blue 0821U	121	208	238
PANTONE®Green 0921U	122	230	207
PANTONE®2239U	0	209	181
PANTONE®2240U	0	194	161
PANTONE®2241U	105	161	147
PANTONE®2242U	0	164	127
PANTONE®2243U	66	149	130
PANTONE®2244U	80	134	122
PANTONE®2295U	221	243	138
PANTONE®2296U	207	239	110
PANTONE®2297U	182	230	74
PANTONE®2298U	166	222	98
PANTONE®2299U	146	212	81
PANTONE®2351U	190	128	179

Supplemental Table 1. Continued.

Sample	R	G	B
PANTONE®2352U	179	112	165
PANTONE®2430U	211	163	127
PANTONE®2438U	226	162	135
PANTONE®2453U	183	145	193
PANTONE®2455U	137	182	172
PANTONE®2464U	112	188	118
PANTONE®2467U	185	155	127
PANTONE®2473U	199	186	191
PANTONE®3506U	97	111	168
PANTONE®3533U	73	210	183
PANTONE®3558U	149	146	205
PANTONE®3568U	248	194	214
PANTONE®3570U	156	205	27
PANTONE®3577U	134	173	208
PANTONE®7408U	231	157	35
PANTONE®7506U	244	225	182
PANTONE®7507U	254	221	169
PANTONE®7508U	219	179	131
PANTONE®7509U	205	162	114
PANTONE®7510U	185	139	95
PANTONE®7548U	255	202	10
PANTONE®7562U	185	160	120

Supplemental Table 2. Root mean square error (RMSE) accuracy scores of each set of 42 measurement points. L*, a*, and b* represent the values on each coordinate axis (lightness, greenness to redness, blueness to yellowness) in the CIE 1976 Lab color space. RMSE scores indicates the magnitude of the difference from the values measured by the colorimeter. The colored values are the lower of the two values, before (bottom side) or after calibration (upper side). The designation "(ref. ROI)" indicates the location of the reference region of interest used for background correction.

L*

	A	B	C	D	E	F	G
1	1.788907	1.784547	1.851416	1.86014	1.826826	1.805568	1.799223
	13.09245	12.23768	11.91849	12.1537	12.45336	12.90863	13.80348
2	1.974661	1.829506	1.866254	1.909674	1.843401	1.849356	1.87905
	12.46337	11.71618	11.35128	11.58611	11.86299	12.47452	13.36537
3	1.945984	1.868838	1.835136	1.847797	1.885382	1.90608	1.85949
	11.9643	11.22644	10.88407	11.13942	11.50594	11.9404	12.90338
				(ref. ROI)			
4	1.868896	1.86836	1.850959	1.872803	1.920099	1.892428	1.907693
	11.93191	11.13296	10.80606	11.16232	11.46168	11.95049	12.67106
5	1.903555	1.845255	1.922859	1.847538	1.810027	1.845676	1.835095
	12.20773	11.44602	11.38607	11.57584	11.97196	12.28159	13.14119
6	1.827756	1.81545	1.843396	1.786399	1.822416	1.888591	1.905774
	13.33698	12.48155	12.47758	12.71891	12.99284	13.5371	14.29716

a*

	A	B	C	D	E	F	G
1	4.974188	5.025764	4.967927	5.065195	5.036866	5.010025	4.976358
	3.218918	3.222332	3.22147	3.23489	3.255033	3.26289	3.227371
2	5.013711	5.005541	5.0259	5.00663	5.075252	5.004309	4.976215
	3.262118	3.219643	3.277016	3.286017	3.269495	3.280423	3.296393
3	4.992217	5.020396	5.048833	5.121253	5.104669	5.066943	4.894878
	3.312489	3.265761	3.342711	3.246253	3.28346	3.400002	3.235783
				(ref. ROI)			
4	5.001611	5.095403	5.055286	5.101401	5.153052	5.008289	4.970854
	3.321639	3.249454	3.282786	3.237006	3.316068	3.316958	3.279464
5	4.970545	5.164807	5.079161	5.030049	4.99424	5.011082	4.989422
	3.307166	3.313216	3.268048	3.287021	3.238975	3.294206	3.21324
6	4.906446	4.995564	4.976752	4.949074	4.915931	4.944481	4.826753
	3.320031	3.288362	3.217873	3.238275	3.253605	3.213292	3.197674

b*

	A	B	C	D	E	F	G
1	3.227352	3.203004	3.375265	3.225724	3.353933	3.145394	3.179588
	4.64098	4.530632	4.461475	4.432125	4.425359	4.45705	4.493107
2	3.438135	3.284865	3.367808	3.194528	3.354539	3.341381	3.290355
	4.554811	4.480996	4.42167	4.335986	4.484412	4.474825	4.515382
3	3.519974	3.620678	3.36614	3.167562	3.215014	3.259561	3.335059
	4.666603	4.418481	4.553116	4.395025	4.406684	4.377068	4.467147
				(ref. ROI)			
4	3.484396	3.391784	3.078657	3.345808	3.313587	3.218625	3.396047
	4.554057	4.385272	4.386327	4.245453	4.338242	4.255381	4.412861
5	3.471848	3.399237	3.087202	2.808967	2.88024	3.205328	3.42591
	4.506401	4.387069	4.296408	4.245779	4.225	4.169605	4.293996
6	3.375723	3.40065	3.197386	3.142025	3.130062	3.335849	3.383038
	4.433448	4.349865	4.302239	4.24342	4.151818	4.192871	4.280444